RNA (2000), *6*:1347–1355. Cambridge University Press. Printed in the USA.

The crystal structure of HIV reverse-transcription primer tRNA(Lys,3) shows a canonical anticodon loop

P. BÉNAS, G. BEC, G. KEITH, R. MARQUET, C. EHRESMANN, B. EHRESMANN, and P. DUMAS

Unité Propre de Recherche 9002 du Centre National de la Recherche Scientifique, Institut de Biologie Moléculaire et Cellulaire, 67084 Strasbourg cedex, France

ABSTRACT

We have solved to 3.3 Å resolution the crystal structure of the HIV reverse-transcription primer tRNA(Lys,3). The overall structure is exactly comparable to the well-known L-shape structure first revealed by yeast tRNA(Phe). In particular, it unambiguously shows a canonical anticodon loop. This contradicts previous results in short RNA fragment studies and leads us to conclude that neither frameshifting specificities of tRNA(Lys) nor tRNA(Lys,3) primer selection by HIV are due to a specific three-dimensional anticodon structure. Comparison of our structure with the results of an NMR study on a hairpin representing a nonmodified anticodon stem-loop makes plausible the conclusion that chemical modifications of the wobble base U34 to 5-methoxycarbonyl-methyl-2-thiouridine and of A37 to 2-methylthio-*N*-6-threonylcarbamoyl-adenosine would be responsible for a canonical 7-nt anticodon-loop structure, whereas the unmodified form would result in a noncanonical UUU short triloop. The hexagonal crystal packing is remarkable and shows tight dimers of tRNAs forming a right-handed double superhelix. Within the dimers, the tRNAs are associated head-to-tail such that the CCA end of one tRNA interacts with the anticodon of the symmetry-related tRNA. This provides us with a partial view of a codon–anticodon interaction and gives insights into the positioning of residue 37, and of its posttranscriptional modifications, relative to the first base of the codon.

Keywords: anticodon; HIV; modified bases; reverse transcription primer; tRNA

INTRODUCTION

Transfer RNA plays a central role in translation of genetic information as a universal "adaptor" between each free amino acid and its codons on any mRNA. Structurally, such a role is well described for all but the last stage on the ribosome, following the numerous studies devoted to all components, either in isolation, or engaged in RNA–protein complexes (see Dirheimer et al., 1995, for tRNAs; Cavarelli & Moras, 1995, Sherman et al., 1995, and Arnez & Moras, 1998, for aminoacyl-tRNA synthetases; Clark & Nyborg, 1997, for EF-Tu; and Auffinger & Westhof, 1999, for a list of crystal structures involving a tRNA). Concerning tRNA interaction with the ribosome machinery, structural information of utmost importance has been available only recently, but at moderate or low resolution (Stark et al., 1997; Cate et al., 1999).

Reprint requests to: P. Dumas, Unité Propre de Recherche 9002 du Centre National de la Recherche Scientifique, Institut de Biologie Moléculaire et Cellulaire, 15 rue René Descartes, 67084 Strasbourg cedex, France; e-mail: P.Dumas@ibmc.u-strasbg.fr.

Furthermore, tRNAs are involved in functions other than the delivering of an amino acid to a growing polypeptide chain. Among these is their use as primers of reverse transcription by infectious retroviruses, as well as by endogenous retroelements (for a review, see Marquet et al., 1995). For HIV, the primer is tRNA(Lys,3) with its 18 3′ end residues being complementary to the primer binding site (PBS) on the viral RNA (Ratner et al., 1985). Additional interactions were found, among which the particularly important one between the UUU tRNA(Lys,3) anticodon and an A-rich loop within the viral RNA 10 residues upstream of the PBS (Isel et al., 1993). Importantly, U34 at the wobble position is modified to 5-methoxycarbonyl-methyl-2-thiouridine (mcm^5s^2U or **S**), a feature that has been recognized as a determinant of this additional interaction, as well as of specificity for efficient initiation of reverse transcription (Isel et al., 1993, 1996). In addition, A37 is modified to 2-methylthio-*N*-6-threonylcarbamoyl-adenosine (ms^2t^6A or $\mathbb{R}$). It has been claimed that both these modifications at U34 and A37 are responsible for an unusual tRNA(Lys,3) anticodon structure due to inter-

action between the modified nucleoside bases (Agris et al., 1997). According to this study, the latter feature would account for both the use of human tRNA(Lys,3) as the HIV primer and the tendency of bacterial and mammalian tRNA(Lys) with **S**UU-like anticodons to frameshift.

As a part of our structural project on initiation of HIV-1 reverse transcription, we have crystallized and solved the structure of mammalian tRNA(Lys,3). At variance with the previous results, our analysis shows a perfectly canonical tRNA with an anticodon fully comparable to those of the refined structures of free elongator tRNAs, namely yeast tRNA(Phe) (Jack et al., 1976; Quigley & Rich, 1976) and tRNA(Asp) (Westhof et al., 1985). Interesting features emerged from the crystal packing. Those include codon–anticodon-like features by the interaction of C75 and A76 of one tRNA with the anticodon of a symmetry-related tRNA.

RESULTS AND DISCUSSION

Overall description of the structure

The primary and secondary structures of tRNA(Lys,3) are shown in Figure 1 (Raba et al., 1979). The overall tertiary structure of tRNA(Lys,3) is fully comparable with the well-known L-shape structure first revealed by yeast tRNA(Phe) (Kim et al., 1973; Robertus et al., 1974). In particular, all usual tertiary interactions are found: the reverse-Hoogsteen base pairs U8•A14 and T_m54•m^{1}A58, the *cis* base pair G18–Ψ55, the *trans* Watson–Crick G15–m^{5}C48 (the so-called "Levitt pair"), the Watson–Crick-like A26–G44, the "U-turns" at U33 and Ψ55, the base triples A9∼(A23–U12), m^{7}G46∼(G22–C13), and G45∼(G10–C25), and finally the Watson–Crick base pair G19–C56 forming the corner of the L. For the latter, however, there is strong evidence of an alternate conformation because G19 also interacts with C56 of a symmetry-related molecule (not shown). Such opening of the corner had been already observed for the B form of yeast tRNA(Asp) (Westhof et al., 1985). Interestingly, the closely related A form was found significantly different at this place with no opening of the G19–C56 base pair (Dumas, 1986). Thus, the present structure confirms that this tertiary base pair is versatile and susceptible to opening.

The anticodon is well defined in the electron-density map (Fig. 2A) and its structure is exactly comparable to the canonical one shown by yeast tRNA(Phe) and tRNA(Asp) (Fig. 3). In particular, the interaction between C32 and A38 corresponds to the general Y32-R38 interaction motif (Auffinger & Westhof, 1999). The modified bases, comprising those in the anticodon, are well visible in the electron-density map despite the rather low resolution of 3.3 Å (Fig. 2A–C).

Only 16 isolated peaks in residual electron density maps [calculated with coefficients $(3F_{Obs} - 2F_{Calc})$] could be safely ascribed to solvent molecules. This is in agreement with the use of the free-*R* index (Brünger, 1992), which is very efficient at preventing "fitting noise" and interpreting spurious peaks as solvent molecules in a rather low resolution structure. One of these peaks, in the major groove of the acceptor stem, was significantly higher than the others (3.5σ above mean level in comparison of 2σ, or less, for those ascribed to water molecules). Therefore, one may suspect that it corresponds to a magnesium site. However, at such resolution, only replacement of magnesium by manganese and confirmation of its binding because of its anomalous scattering signature would provide a firm conclusion.

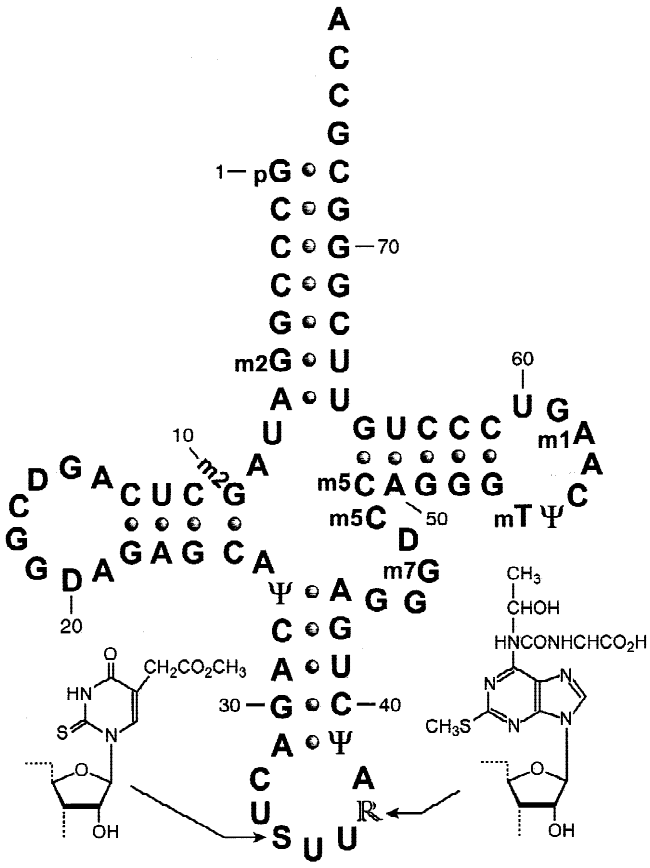

FIGURE 1. Primary and secondary structures of mammalian tRNA(Lys,3) highlighting the modified residues mcm^{5}s^{2}U34 (**S**34) and ms^{2}t^{6}A37 (ℝ37).

A remarkable crystal packing

The crystal packing is remarkable. First, two tRNAs are closely associated head-to-tail so that the CCA end of each one interacts with the anticodon of the other one (Fig. 4). Second, such dimers form a right-handed double superhelix, roughly 70 Å in diameter (Fig. 5), with a rather unusual interaction of two symmetry-related pairs of anticodon–CCA (Fig. 6). As a result,

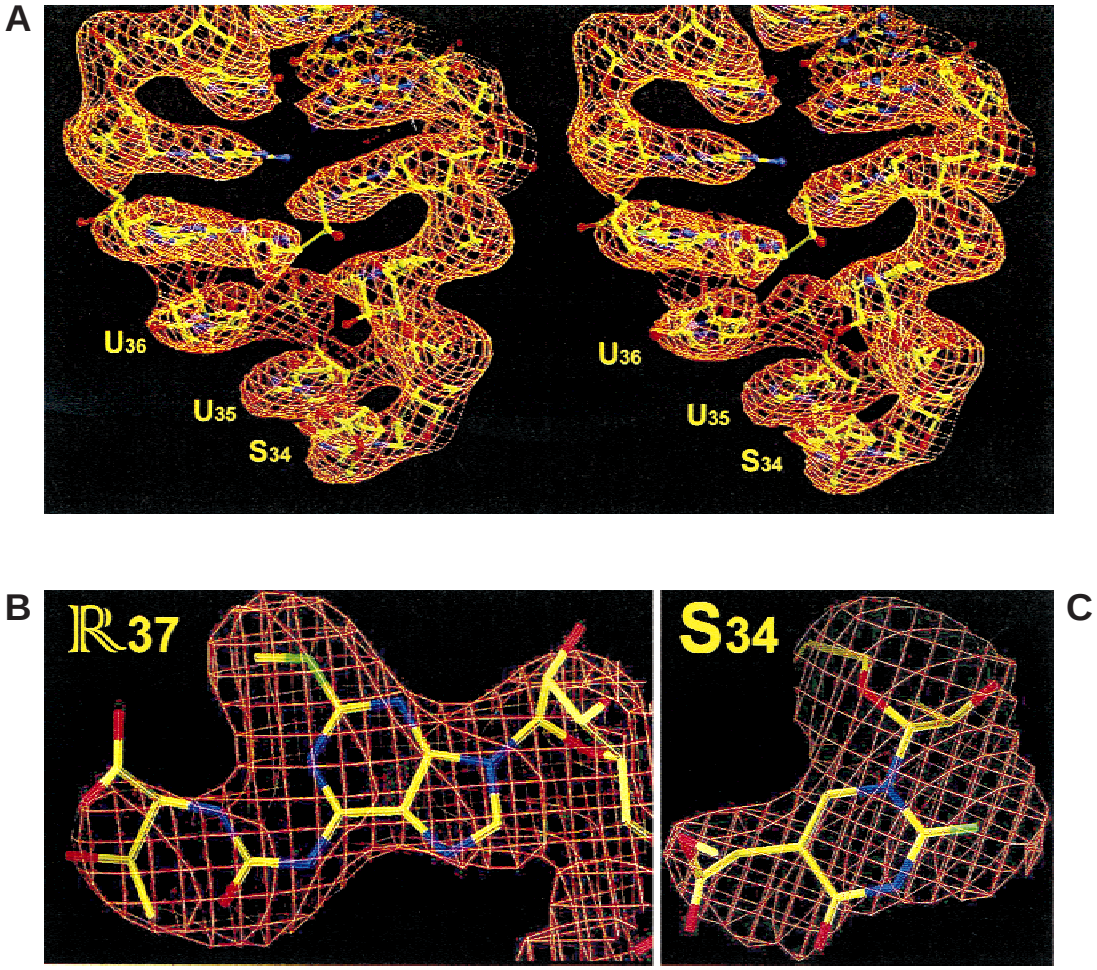

FIGURE 2. Electron density map around anticodon and around bases with chemical modifications. **A**: General stereo-view of the anticodon loop showing perfect canonical 3′ end stacking. **B**: Detailed view of ℝ37. **C**: Detailed view of **S**34.

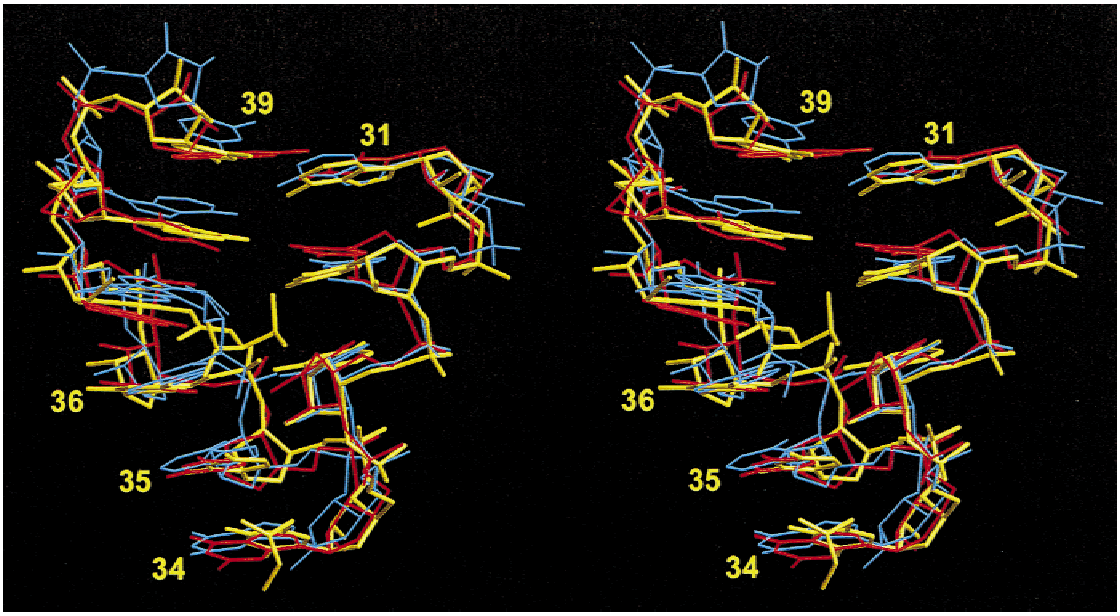

FIGURE 3. Comparison of tRNA(Lys,3) (yellow), tRNA(Phe) (PDB 4TNA, blue), and tRNA(Asp) (PDB 2TRA, red) anticodons.

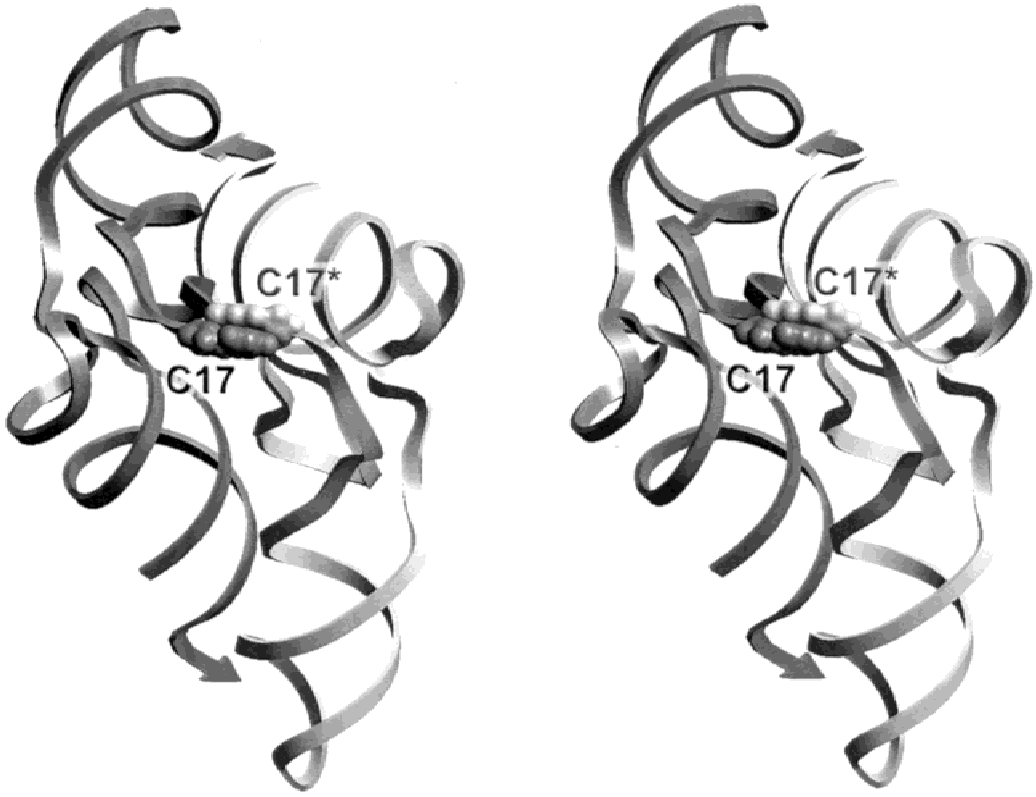

FIGURE 4. General stereo-view of the head-to-tail interaction with the two stacked C17s highlighted.

one has the impression of two anticodons ready to form an anticodon–anticodon interaction, but prevented from doing so by the two CCAs arriving in opposite orientation. The interaction between a CCA and a symmetry-related anticodon involves the formation of a noncanonical, and quite unusual, C75–U36* base pair (the asterisk marks the twofold symmetry in the head-to-tail interaction). Rather oddly, A76 is only close to form an A76–U35* Watson–Crick base pair that would naturally follow the C75–U36* base pair, but instead forms a Hoogsteen-type interaction with **S**34$^{\#}$ (the # marks the twofold symmetry relating the dimers). In case of an isolated dimer, that is, with no U34$^{\#}$ available, the latter A76•U34$^{\#}$ Hoogsteen interaction would certainly be replaced by the almost formed A76–U35* Watson–Crick base pair. Finally, the other nonionic interactions stabilizing each dimer involve stacking of C17 onto its symmetry mate C17* (Fig. 4). Overall, each dimer is stabilized by four base–base interactions involving either hydrogen bonds or stacking of aromatic rings.

This packing interaction involving a CCA and an anticodon is interesting as the C75–U36* base pair and the almost formed A76–U35* base pair give a significant partial view of a codon–anticodon interaction (although C75–U36* is not a relevant base pair at this place, the position occupied by the pyrimidine ring of C75 is exactly that of a complementary adenine six-membered ring) (Fig. 6). Clearly, the interaction seen in this case is not as suggestive of a codon–anticodon interaction as the one seen in yeast tRNA(Asp) crystals (Westhof et al., 1985; Moras et al., 1986) but, nevertheless, it gives insight into the mutual position of the modified base 37 versus the first base of the interacting codon (see below). It can also be mentioned that the two stacked U34$^{\#}$•A76∼U35* motifs, where the ∼ marks the almost formed Watson–Crick base pair between A76 and U35* (Fig. 6), are strikingly similar to the two stacked C^{+}•G-C motifs seen in the crystal structure of a DNA triple helix (Rhee et al., 1999).

It is likely that this dimeric form (Fig. 4) is the building unit of the crystal and, therefore, exists in solution. Clearly, in crystallization drops, the 1.6 M lithium sulfate high ionic strength allows efficient screening of the negatively charged phosphates and stabilizes the association. Under usual physiological conditions, involving concentrations of ∼0.1 M monovalent cations and a 5–10 mM range for Mg^{2+}, the dimer might not be stable enough. However, for halophilic bacteria living in 20–25% (w/v) salt concentration, the possibility that such dimers exist should not be rejected. Considering that their stabilization requires binding of C75 and A76 to the bases 36 and 35 of an anticodon, and if one accepts an A76–G35 pairing (either as a Watson–Crick-like, or as a sheared base pair) in addition to A76–U35, one comes to tRNAs with four possible anticodon types:

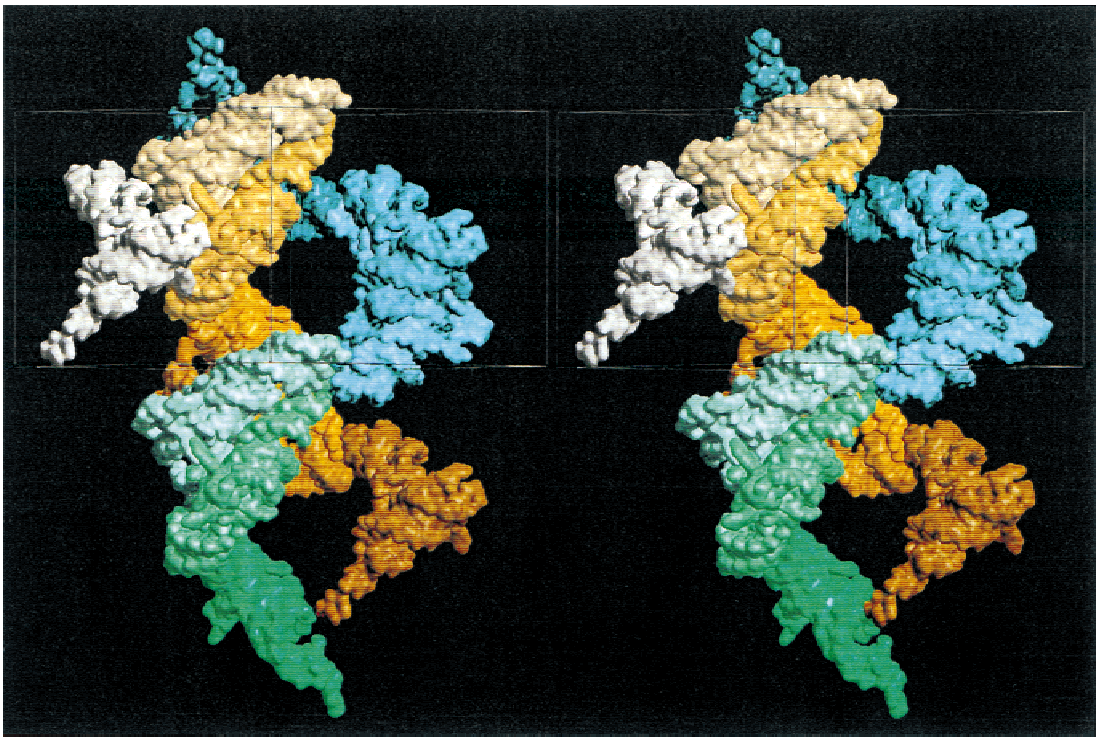

FIGURE 5. General stereo-view of the right-handed double helix of dimers shown in Figure 4. For the sake of clarity, only one tRNA (in white) involved in contacts between superhelix strands has been shown.

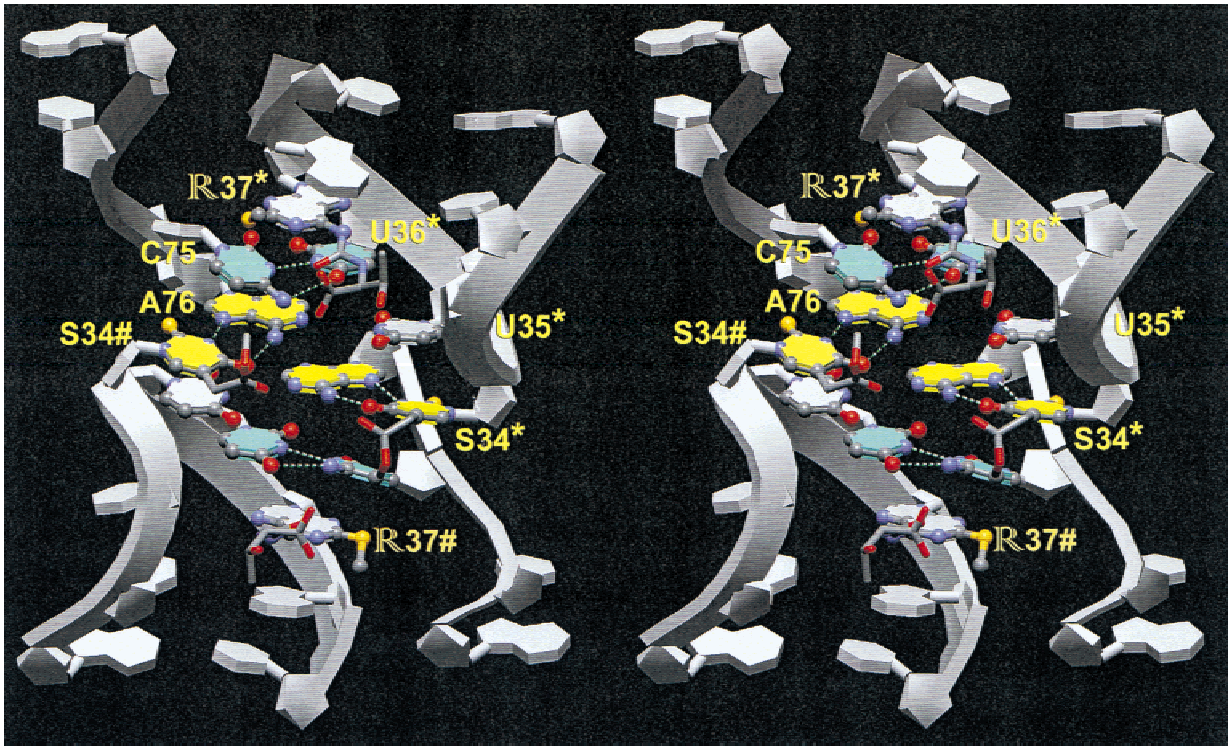

FIGURE 6. Detailed stereo-view around the anticodon–CCA interaction showing the two symmetry-related CCAs arriving in opposite orientation within a short triple helix. The noncanonical base pair C75–U36* (and its symmetrical) are shown in blue, and the Hoogsteen base pair A76•**S**34# (and its symmetrical) are shown in yellow. Note how the latter Hoogsteen base pair maintains A76 too far away from U35* to form a Watson–Crick interaction.

X34 (U/G)35 (U/G)36. These correspond essentially to tRNAs for Asn, His, Lys, Pro, Thr, and Gln, which, apart from tRNA(Gln), are all substrates of a dimeric class II aminoacyl-tRNA synthetase. If this is not coincidental, it may be thought that such tRNA dimerization could increase the rate of binding to a dimeric aaRS requiring two tRNA substrates.

Description of the anticodon with regards to modifications at U34 and A37

Chemical modifications at 34 and 37 appear clearly and do not present, as previously proposed by others, either mutual interactions (Agris et al., 1997) or any other unusual feature that could explain the different behavior of tRNA(Lys) versus tRNA(Glu) from *Escherichia coli* (Watanabe et al., 1993). What is seen for **S**34 is the perfect stacking of its O2-replacing sulfur onto the aromatic ring of U35 (Fig. 6). This is not unexpected when considering the well-known stabilizing effect of 2-thio modification (Watanabe et al., 1979; Yokoyama et al., 1979, 1985; Houssier et al., 1988; Kumar & Davis, 1997; Grosjean et al., 1998). Less expected, however, is the pronounced stacking of the threonylcarbamoyl moiety of ℝ37 onto A38, and not onto U36 as previously thought (Parthasarathy et al., 1974, 1977). Interestingly, the sulfur of the thiomethyl group on the same ℝ37 is stacked onto C75 of the symmetry-related molecule within a dimer. That this crystal packing feature can be viewed, as explained above, as a part of a codon–anticodon interaction gives a reasonable view of the positioning of both A37-modifying chemical groups during codon reading by tRNA(Lys,3). This will be discussed elsewhere in view of tRNA(Lys) and other tRNAs frameshifting abilities.

Comparison with NMR studies

The canonical anticodon structure that we observe contrasts with previous results of two NMR studies. These differences cannot be reconciled with the results of the first work (Agris et al., 1997) but, apparently, correspond to genuine features in the second case (Durant & Davis, 1999). The first NMR study (Agris et al., 1997) concerned a pentanucleotide encompassing the anticodon residues from U33 to A37, with U34 and A37 present as their modified form **S**34 and ℝ37, respectively. The result of this work is that the side chains of **S**34 and ℝ37 interact. According to the authors, this would prevent the tRNA(Lys,3) anticodon loop from having a canonical conformation. However, such contradiction with our finding certainly results from their use of a pentanucleotide, instead of a relevant heptanucleotide loop locked by at least 2 bp. It seems difficult, indeed, to argue that the conformation that we describe results from intermolecular contacts in the crystal, and that a free tRNA(Lys,3) would have a noncanonical anticodon conformation. Doing so would merely amount to invoking a "packing artifact" to explain why the expected canonical, and functional, conformation has been obtained.

For the second solution study (Durant & Davis, 1999), on the contrary, the fragment was much longer (17 nt) and certainly representative of an anticodon loop. A noticeable feature of their RNA fragment is that it was devoid of modifications at U34 and A37. This gave this model molecule the characteristics of a hypomodified tRNA(Lys,3). The result of this work, essentially, is that there is departure from a canonical anticodon loop conformation with (1) formation of a U33–A37 base pair (and of a C32–A^{+}38 base pair at pH 5), (2) absence of the usual U-turn at U33, and (3) deviation from A-form geometry for the three Us of the anticodon that become very mobile with their ribose having a significant C2′-endo character. It should be noted that points (1), (2), and (3) would agree equally well with a duplex having three consecutive, more or less melted, U–U base pairs. However, Durant and Davis (1999) have considered such a possibility and, on the basis of spectroscopic data at various temperatures, concluded the absence of significant amounts of the duplex form for this unmodified sequence (but, noticeably, they detected the duplex form when U34 was replaced by a 2-thiouridine). As such, it is thus reasonable to consider that the latter NMR structure corresponds to an unusual tRNA(Lys,3) anticodon loop resulting from hypomodification, whereas the crystal structure reported here corresponds to the canonical anticodon loop of the fully modified tRNA(Lys,3). In support of this interpretation, it has been shown that an unmodified transcript of tRNA(Lys,3), as well as an unmodified anticodon loop-mimicking hairpin, do not bind to an AAA or AAG-programmed ribosome, whereas thiolation of the U34-mimicking U in the hairpin restores its binding (Ashraf et al., 1999).

CONCLUSION

The main conclusion from the present study is that a classical tRNA(Lys,3) anticodon is formed. This is all but surprising in view of the unique stereochemical requirements imposed by the ribosome machinery on all elongator tRNAs. In addition, tRNA(Lys,3) has been selected as the HIV reverse-transcription primer. For that rather unusual function, two unrelated specificities are required. First, its 18 3′ end residues must be complementary with the PBS on HIV genomic RNA (Ratner et al., 1985). Second, it has been shown that its anticodon loop must be complementary with an A-rich loop close to the PBS (Isel et al., 1993). Furthermore, an NMR study has shown that the latter A-rich loop has a classical anticodon-like structure (Puglisi & Puglisi, 1998). Again, as already pointed out by Durant and Davis (1999), this calls very strongly for a canonical

tRNA(Lys,3) anticodon loop structure, as two such complementary loops can readily interact (Grosjean et al., 1978; Moras et al., 1986). Therefore, for its elongator function, as well as for its HIV primer function, a canonical anticodon loop is certainly the relevant one. Thus, in contradiction with previous claims (Agris et al., 1997), it appears that none of the tRNA(Lys,3) functional specificities is to be explained by a peculiar and preexisting three-dimensional anticodon structure. In particular, the fact that this tRNA is used as the reverse-transcription primer by HIV must be found in its primary sequence (including the chemical modification at U34) allowing it to form an extremely specific complex with the viral RNA (Isel et al., 1995, 1999). Evidently, one cannot exclude that some unknown abnormal folding of this tRNA could facilitate its hybridization to the PBS.

MATERIALS AND METHODS

tRNA purification

tRNA(Lys,3) was purified from beef, rabbit, and even chicken liver, as all three sequences, including their posttranscriptional modifications, are identical to those of human tRNA(Lys,3) (G. Keith, unpubl. data). The following procedure derived from Keith et al. (1983) was used and yielded in the best cases 10–20 mg of pure material. Nucleic acids were phenol extracted from ~30 kg of liver tissue, then submitted to a fractionated precipitation between 20% and 42% (v/v) isopropanol and eluted from a batchwise adsorption on DEAE-cellulose using a procedure adapted from Fournier et al. (1976). RNA was ethanol precipitated and extracted by acid guanidinium thiocyanate-phenol-chloroform as described in Chomczynski & Sacchi (1987). Nucleic acids (typically 10 g) were then submitted to BD-cellulose chromatography and eluted by a gradient of NaCl in a 10 mM sodium-acetate buffer, pH 4.5, containing 10 mM $MgCl_2$. tRNA(Lys,3)-containing fractions (eluted between 0.7 and 0.9 M NaCl) were pooled, ethanol precipitated, and applied onto a Sepharose 4B column. Elution by a decreasing ammonium sulfate gradient was performed as described in Keith et al. (1983). In the next step, the ethanol-precipitated tRNA(Lys,3) fractions were applied onto a Poly-A sepharose column equilibrated in 15 mM sodium cacodylate, pH 7.5, 75 mM NaCl, and 750 mM $(NH_4)_2SO_4$. The column was washed with water and the tRNA(Lys,3), bound to the polyA chains by its anticodon, was eluted with 90% formamide (v/v), 20 mM sodium cacodylate, pH 7.5, and 10 mM EDTA. The tRNA(Lys,3) was ethanol precipitated and finally purified on a Mono-Q column (HR 10/10, Pharmacia) using a linear gradient of NaCl (between 450 and 600 mM) in a 20 mM Bis-Tris buffer, pH 6.8.

Crystallization and crystals characterization

tRNA(Lys,3) at an initial concentration of 5 mg/mL was crystallized by the vapor diffusion method at 20 °C in conditions close to one set up from the Natrix kit (Hampton Research). These involved 50 mM MES-KOH, pH 5.6, 10 mM $MgCl_2$ and 1.6–1.8 M Li_2SO_4 as a precipitating agent. Crystals grew up to 400 μm within 2–4 days with two types of habit. One, with a regular prismatic shape, diffracted to about 8 Å resolution. The other one, with concave faces, diffracted to 4.5–4.0 Å in general. Occasionally, for ~2% of them, crystals were found that diffracted up to 3.3 Å resolution. They belonged to space group $P3_212$ with cell dimensions $a = b = 100.7$ Å, $c = 82.6$ Å and, despite a particularly high solvent content of 79%, they were mechanically robust. Due to the presence of concave faces, the possibility of merohedral twinning that could have adversely affected the measured intensities was checked (Yeates, 1997; Dumas et al., 1999). It was concluded that the crystals were not twinned, which was further confirmed by successful molecular replacement and structure refinement.

Data collection, structure solution, and refinement

Crystals were successfully frozen without any additional cryoprotectant either in a nitrogen gas stream or in liquid ethane. A data set has been collected on a single frozen crystal maintained at 110 K on beam line D2AM at the European Synchrotron Radiation Facility (Table 1). Structure solution was carried out by molecular replacement, using AMoRe (Navaza, 1994). A clear solution was obtained with the structure of tRNA(Phe) as a model (PDB code 4TNA) (Table 2A). No clear solution could be obtained when using the structure of tRNA(Asp) (PDB codes 2TRA, 3TRA); this is in agreement with the fact that the overall tRNA(Lys,3) structure is better superimposed onto tRNA(Phe) than onto tRNA(Asp). Model building was performed with O (Jones et al., 1991) and refinement with CNS (Brünger et al., 1998) (Table 2B). For the latter, it was necessary to add new entries into topological and energetic parameters files for the nonstandard modified residues (**S**34, $\mathbb{R}$37, T_m54). An interesting point can be noticed about bulk solvent correction in refinement. Effectively, it was found that the best molecular mask used to delineate the solvent region was, by far, one using a deliberately enlarged molecular volume (by inflating by 5 to 6 Å the strict molecular surface). When the molecular surface was "accurately" defined in CNS by the solvent-accessible surface, re-

TABLE 1. Crystallographic data.

Space group	$P3_212$
Cell parameters (Å)	$a = 100.7$, $c = 82.6$
Cryo conditions	liquid ethane
Mosaicity	1.44°
Resolution range (Å)	25–3.30
Outermost shell (Å)	3.42–3.30
Completeness (outermost shell)	88.2% (71.6%)
$\langle I/\sigma \rangle$ (outermost shell)	10.5 (4.3)
Redundancy (outermost shell)	3.2 (2.2)
Number of unique reflections	6,482
R_{sym}[a] (outermost shell)	8.1% (16.5%)
V_m (Å^3/Da)	5.12
Solvent content	78.7%

[a] $R_{sym} = \langle \sum |I_{h,i} - \langle I_h \rangle| / \sum I_{h,i} \rangle$, where $I_{h,i}$ is the value of the ith measurement of the intensity of the hth reflection, and $\langle I_h \rangle$ is the average value of these observations. The summation is made from $i = 1$ to the number of observations for that hth reflection and the overall average is calculated on all reflections.

TABLE 2A. Structure solution by molecular replacement.[a]

Models		First solution	Second solution
tRNA(Asp) (2TRA)	Correlation factors	27.5%	26.4%
	R factors	48.0%	48.4%
tRNA(Phe) (4TNA)	Correlation factors	**43.4%**	**23.7%**
	R factors	44.5%	51.8%

[a]Resolution range (Å): 10–5.0.

TABLE 2B. Statistics after refinement.

Resolution range (Å)	25–3.3
% of test reflections	8.0%
Free *R*-factor	24.0%
R-factor	20.3%
R.m.s.d bond lengths (Å)	0.01
R.m.s.d bond angles (degrees)	1.6
Estimated error on coord. (Å)	0.36
Average *B* factor (Å^2)	35
No. of nucleic acid atoms	1,645
No. of solvent molecules	16

finement statistics were markedly affected. Our interpretation is that the accurate mask added, in fact, spurious details to the solvent contribution. In some way, the enlarged and thus smoother mask provided an efficient resolution-dependent weighting of that contribution. This remains, however, to be proven. Furthermore, this might be restricted to refinements of structures with large solvent content only.

NOTE ADDED IN PROOFS

Coordinates have been deposited with the Nucleic Acids Data Base (ID: TR0003) and with the Protein Data Bank (ID: 1FIR).

ACKNOWLEDGMENTS

This work has been supported by grants from the "Association Nationale de la Recherche sur le SIDA" and by the "Association de Recherche sur le Cancer." We are grateful to C. Fix for help in tRNA purification, E. Ennifar for help in data collection, and M. Gaine for excellent technical assistance. E. Fanchon and M. Roth are greatly acknowledged for their help on beam line D2AM at ESRF(Grenoble).

Received May 5, 2000; returned for revision June 6, 2000; revised manuscript received June 26, 2000

REFERENCES

Agris PF, Guenther R, Ingram PC, Basti MM, Stuart JW, Sochacka E, Malkiewicz A. 1997. Unconventional structure of tRNA(Lys)SUU anticodon explains tRNA's role in bacterial and mammalian ribosomal frameshifting and primer selection by HIV-1. *RNA 3*:420–428.

Arnez JG, Moras D. 1998. tRNA/Aminoacyl-tRNA synthetase interactions. In: Simons RW, Grunberg-Manago M, eds. *RNA structure and function*. Cold Spring Harbor, New York: Cold Spring Harbor Laboratory Press. pp 465–494.

Ashraf SS, Sochacka E, Cain R, Guenther R, Malkiewicz A, Agris PF. 1999. Single atom modification (O → S) of tRNA confers ribosome binding. *RNA 5*:188–194.

Auffinger P, Westhof E. 1999. Singly and bifurcated hydrogen-bonded base-pairs in tRNA anticodon hairpins and ribozymes. *J Mol Biol 292*:467–483.

Brünger AT. 1992. The free R value: A novel statistical quantity for assessing the accuracy of crystal structures. *Nature 335*:472–474.

Brünger AT, Adams PD, Clore GM, DeLano WL, Gros P, Grosse-Kunstleve RW, Jiang JS, Kuszewski J, Nilges M, Pannu NS, Read RJ, Rice LM, Simonson T, Warren GL. 1998. Crystallography & NMR system: A new software suite for macromolecular structure determination. *Acta Cryst D54*:905–921.

Cate J, Yusupov M, Yusupova G, Earnest T, Noller H. 1999. X-ray crystal structures of 70S ribosome functional complexes. *Science 285*:2095–2104.

Cavarelli J, Moras D. 1995. The aspartic acid tRNA system: Recognition by a Class II aminoacyl-tRNA synthetase. In: Söll D, RajBhandary UL, eds. *tRNA: Structure, biosynthesis and function*. Washington, DC: ASM Press. pp 411–422.

Chomczynski P, Sacchi N. 1987. Single-step method of RNA isolation by acid guanidinium thiocyanate-phenol-chloroform extraction. *Anal Biochem 162*:156–159.

Clark BFC, Nyborg J. 1997. The ternary complex of EF-Tu and its role in protein biosynthesis. *Curr Opinion Struc Biol 7*:110–116.

Dirheimer G, Keith G, Dumas P, Westhof E. 1995. Primary, secondary and tertiary structures of tRNAs. In: Söll D, RajBhandary UL, eds. *tRNA: Structure, biosynthesis and function*. Washington, DC: ASM Press. pp 93–126.

Dumas P. 1986. Affinement cristallographique et étude structurale de l'ARN de transfert de levure spécifique de l'acide aspartique, Thèse d'Etat de l'Université Louis Pasteur-Strasbourg (France).

Dumas P, Ennifar E, Walter P. 1999. Detection and treatment of twinning: An improvement and new results. *Acta Cryst D55*: 1179–1187.

Durant PC, Davis DR. 1999. Stabilization of the anticodon stem-loop of tRNA(3Lys) by an A^+-C base-pair and by pseudouridine. *J Mol Biol 285*:115–131.

Fournier M, Dorizzi M, Sarger C, Labouesse J. 1976. Purification of tRNATrp, tRNAVal, and partial purification of tRNAIle and tRNAfMet from beef liver. *Biochimie 58*:1159–1165.

Grosjean H, de Henau S, Crothers DM. 1978. On the physical basis for ambiguity in genetic coding interactions. *Proc Natl Acad Sci USA 75*:610–614.

Grosjean H, Houssier C, Romby P, Marquet R. 1998. Modulatory role of modified nucleotides in RNA loop–loop interaction. In: Grosjean H, Benne R, eds. *Modification and editing of RNA*. Washington, DC: ASM Press. pp 113–133.

Houssier C, Degee P, Nicoghosian K, Grosjean H. 1988. Effect of uridine dethiolation in the anticodon triplet of tRNA(Glu) on its association with tRNA(Phe). *J Biomol Struct Dyn 5*:1259–1266.

Isel C, Ehresmann C, Keith G, Ehresmann B, Marquet R. 1995. Initiation of reverse transcription of HIV-1: Secondary structure of the HIV-1 RNA/tRNA(Lys,3) (template/primer). *J Mol Biol 247*: 236–250.

Isel C, Lanchy JM, Le Grice SF, Ehresmann C, Ehresmann B, Marquet R. 1996. Specific initiation and switch to elongation of human immunodeficiency virus type 1 reverse transcription require the post-transcriptional modifications of primer tRNA(Lys,3). *EMBO J 15*:917–924.

Isel C, Marquet R, Keith G, Ehresmann C, Ehresmann B. 1993. Modified nucleotides of tRNA(3Lys) modulate primer/template loop–loop interaction in the initiation complex of HIV-1 reverse transcription. *J Biol Chem 268*:25269–25272.

Isel C, Westhof E, Massire C, Le Grice SF, Ehresmann B, Ehresmann C, Marquet R. 1999. Structural basis for the specificity of the initiation of HIV-1 reverse transcription. *EMBO J 18*:1038–1048.

Jack A, Ladner JE, Klug A. 1976. Crystallographic refinement of yeast phenylalanine transfer RNA at 2.5 Å resolution. *J Mol Biol 108*:619–649.

Jones TA, Zhou JY, Cowan SW, Kjeldgaard M. 1991. Improved methods for the building of protein models in electron density maps and the location of errors in these models. *Acta Cryst A47*:110–119.

Keith G, Pixa G, Fix C, Dirheimer G. 1983. Primary structure of three tRNAs from brewer's yeast: tRNA(Pro,2), tRNA(His,1) and tRNA(His,2). *Biochimie 65*:661–672.

Kim SH, Quigley GJ, Suddath FL, McPherson A, Sneden D, Kim JJ, Weinzierl J, Rich A. 1973. Three-dimensional structure of yeast phenylalanine transfer RNA: Folding of the polynucleotide chain. *Science 179*:285–288.

Kumar RK, Davis DR. 1997. Synthesis and studies on the effect of 2-thiouridine and 4-thiouridine on sugar conformation and RNA duplex stability. *Nucleic Acids Res 25*:1272–1280.

Marquet R, Isel C, Ehresmann C, Ehresmann B. 1995. tRNAs as primer of reverse transcriptases. *Biochimie 77*:113–124.

Moras D, Dock AC, Dumas P, Westhof E, Romby P, Ebel JP, Giege R. 1986. Anticodon-anticodon interaction induces conformational changes in tRNA: yeast tRNAAsp, a model for tRNA–mRNA recognition. *Proc Natl Acad Sci USA 83*:932–936.

Navaza J. 1994. AMoRe: An automated package for molecular replacement. *Acta Cryst A50*:157–163.

Parthasarathy R, Ohrt JM, Chheda GB. 1974. Conformation of N-(purin-6ylcarbamoyl) glycine, a hypermodified base in tRNA. *Biochem Biophys Res Commun 57*:649–653.

Parthasarathy R, Ohrt JM, Chheda GB. 1977. Modified nucleosides and conformation of anticodon loops: Crystal structure of t6A and g6A. *Biochemistry 16*:4999–5008.

Puglisi EV, Puglisi JD. 1998. HIV-1 A-rich RNA loop mimics the tRNA anticodon structure. *Nat Struct Biol 5*:1033–1036.

Quigley GJ, Rich A. 1976. Structural domains of transfer RNA molecules. *Science 194*:796–806.

Raba M, Limburg K, Burghagen M, Katze JR, Simsek M, Heckman JE, Rajbhandary VL, Gross HJ. 1979. Nucleotide sequence of three isoaccepting lysine tRNAs from rabbit liver and SV40-transformed mouse fibroblasts. *Eur J Biochem 97*:305–318.

Ratner L, Haseltine W, Patarca R, Livak KJ, Starcich B, Josephs SF, Doran ER, Rafalski JA, Whitehorn EA, Baumeister K, Ivanoff L, Petteway SRJ, Pearson ML, Lautenberger JA, Papas TS, Ghrayeb J, Chang NT, Gallo RC, Wong-Staal F. 1985. Complete nucleotide sequence of the AIDS virus, HTLV-III. *Nature 313*:277–284.

Rhee S, Han ZJ, Liu K, Miles T, Davies DR. 1999. Structure of a triple helical DNA with a triplex-duplex junction. *Biochemistry 38*:16810–16815.

Robertus JD, Ladner JE, Finch JT, Rhodes D, Brown RS, Clark BF, Klug A. 1974. Structure of yeast phenylalanine tRNA at 3 Å resolution. *Nature 250*:546–551.

Sherman JM, Rogers MJ, Söll D. 1995. Recognition in the Glutamine tRNA system: From structure to function. In: Söll D, RajBhandary UL, eds. *tRNA: Structure, biosynthesis and function*. Washington, DC: ASM Press. pp 395–409.

Stark H, Rodnina MV, Rinke-Appel J, Brimacombe R, Wintermeyer W, van Heel M. 1997. Visualization of elongation factor-Tu on the *Escherichia coli* ribosome. *Nature 389*:403–406.

Tsuchihashi Z, Brown PO. 1992. Sequence requirements for efficient translational frameshifting in the *Escherichia coli* dnaX gene and the role of an unstable interaction between tRNA(Lys) and an AAG lysine codon. *Genes & Dev 6*:511–519.

Watanabe K, Hayashi N, Oyama A, Nishikawa K, Ueda T, Miura K. 1993. Unusual anticodon loop structure found in *E. coli* lysine tRNA. *Nucleic Acids Res 22*:79–87.

Watanabe K, Yokoyama S, Hansske F, Kasai H, Miyazawa T. 1979. CD and NMR studies on the conformational thermostability of 2-thioribothymidine found in the TψC loop of thermophile tRNA. *Biochem Biophys Res Commun 91*:671–677.

Westhof E, Dumas P, Moras D. 1985. Crystallographic refinement of yeast aspartic acid transfer RNA. *J Mol Biol 184*:119–145.

Yeates TO. 1997. Detecting and overcoming crystal twinning. *Methods Enzymol 276*:344–358.

Yokoyama S, Watanabe T, Murao K, Ishikura H, Yamaizumi Z, Nishimura S, Miyazawa T. 1985. Molecular mechanism of codon recognition by tRNA species with modified uridine in the first position of the anticodon. *Proc Natl Acad Sci USA 82*:4905–4909.

Yokoyama S, Yamaizumi Z, Nishimura S, Miyazawa T. 1979. 1H NMR studies on the conformational characteristics of 2-thiopyrimidine nucleotides found in transfer RNAs. *Nucleic Acids Res 6*:2611–2626.